

VSOP Observations of a Sub-Parsec Accretion Disk

D.L. JONES, A.E. WEHRLE, B.G. PINER & D.L. MEIER

Jet Propulsion Laboratory, California Institute of Technology, USA

Abstract

The physical conditions in the inner parsec of accretion disks believed to orbit the central black holes in active galactic nuclei can be probed by imaging the absorption of background radio emission by ionized gas in the disk. We report high angular resolution observations of the nearby galaxy NGC 4261 which show evidence for free-free absorption by a thin, nearly edge-on disk at several frequencies. The angular width, and probably the depth, of the absorption appears to increase with decreasing frequency, as expected. Because free-free absorption is much larger at lower frequencies, the longest possible baselines are needed to provide adequate angular resolution; observing at higher frequencies to improve resolution will not help.

1 Introduction

The nearby FR-I radio galaxy NGC 4261 (3C270) is a good candidate for the detection of free-free absorption by ionized gas in an inner accretion disk. The galaxy is known to contain a central black hole with a mass of $5 \times 10^8 M_{\odot}$, a nearly edge-on nuclear disk of gas and dust with a diameter of ≈ 100 pc, and a large-scale symmetric radio structure which implies that the radio axis is close to the plane of the sky. At an assumed distance of 40 Mpc, 1 milliarcsecond (mas) corresponds to 0.2 pc. Previous VLBA observations of this galaxy revealed a parsec-scale radio jet and counterjet aligned with the kpc-scale jet (see Figure 1). The opening angle of the jets is less than 20° during the first 0.2 pc and $< 5^{\circ}$ during the first 0.8 pc. At 8.4 GHz we found evidence for a narrow gap in radio brightness at the base of the parsec-scale counterjet, just east (left) of the brightest peak which we identified as the core based on its inverted spectrum between 1.6 and 8.4 GHz (see the left part of Figure 2, from Jones and Wehrle 1997). We tentatively identified this gap as the signature of free-free absorption by a nearly-edge on inner disk with a width $\ll 0.1$ pc and an average electron density of $10^3 - 10^8 \text{ cm}^{-3}$ over the inner 0.1 pc.

Figure 1: VLBA image of NGC 4261 at 8.4 GHz. The contours increase in steps of $\sqrt{2}$ starting at $\pm 0.75\%$ of the peak, which is 99 mJy/beam. The restoring beam is 1.86×0.79 mas with major axis PA = -1.3° .

2 Observations

We observed NGC 4261 at 1.6 and 4.9 GHz with HALCA and a ground array composed of 7 VLBA antennas plus Shanghai, Kashima, and the DSN 70-m Tidbinbilla antennas at 1.6 GHz (22 June 1999) and 8 VLBA antennas plus the phased VLA at 4.9 GHz (27 June 1999). During both epochs the VLBA antennas at St. Croix and Hancock were unavailable, as was the North Liberty antenna at 1.6 GHz. Data were recorded as two 16-MHz bandwidth channels with 2-bit sampling by the Mark-III/VLBA systems and correlated at the VLBA processor in Socorro. Both channels were sensitive to left circular polarization.

Fringe-fitting was carried out in AIPS after applying *a priori* amplitude calibration. For VLBA antennas we used continuously measured system temperatures, for the VLA we used measured T_A/T_{SYS} values with an assumed source flux density of 5 Jy, and for the remaining antennas we used typical gain and system temperature values obtained from the VSOP web site. Fringes were found to all antennas at 1.6 GHz except HALCA, but the signal/noise ratio to Shanghai and Kashima was very low and these data were not used. The *a priori* amplitude calibration for Tidbinbilla was dramatically incorrect for unknown reasons. We calibrated Tidbinbilla by imaging the compact structure of the source using VLBA data, then holding the VLBA antenna gains fixed and allowing the Tidbinbilla gain to vary. This produced a good match in

correlated flux density where the projected VLBA and Tidbinbilla baselines overlap. At 4.9 GHz fringes were found to all antennas, including HALCA. A similar correction to the *a priori* amplitude calibration for HALCA and the phased VLA was applied.

In both observations we found that averaging in frequency over both 16-MHz channels in AIPS produced large, baseline-dependent amplitude reductions even though the post-fringe-fit visibility phases were flat and continuous between channels. Averaging over frequency within each 16-MHz band separately fixed this problem. Difmap was used for detailed data editing, self-calibration, and image deconvolution. Both 16-MHz bands were combined during imaging.

Imaging within Difmap used uniform weighting with the weight of HALCA data increased by a factor of 500. Several iterations of phase-only self calibration, followed by amplitude self calibration iterations with decreasing time scales, resulted in good fits ($\chi^2 \approx 1$) between the source model and the data.

3 Results

3.1 1.6 GHz

Although our image at 1.6 GHz does not include data from HALCA, it does have more than twice the angular resolution of our previous 1.6 GHz image (Jones and Wehrle 1997) due to the addition of Tidbinbilla. The previous image showed a symmetric structure, with the jet and counterjet extending west and east from the core. No evidence for absorption is seen in this image. However, with higher resolution we do detect a narrow gap in emission just east of the core, at the base of the counterjet. The width of the gap is less than 2 mas.

3.2 4.9 GHz

We detected fringes to HALCA at 4.9 GHz when the projected Earth-space baselines were less than one Earth diameter. The HALCA data fills in the (u,v) coverage hole between continental VLBA baselines and those to Mauna Kea, and also increases the north-south resolution by a factor of two. Our 4.9 GHz image is shown in Figure 2. Note that the gap in emission is again seen just east of the peak. A careful comparison of brightness along the radio axis at 4.9 and 8.4 GHz shows that the gap is both deeper and wider at 4.9 GHz, as expected from free-free absorption. The region of the gap has a very inverted spectrum, the brightest peak

Figure 2: Grey-scale images of the nucleus of NGC 4261 at 8.4 GHz (left) and 4.9 GHz (right), with identical fields of view.

(core) has a slightly less inverted spectrum, and the distant parts of both the jet and counterjet have steep spectra.

4 Summary

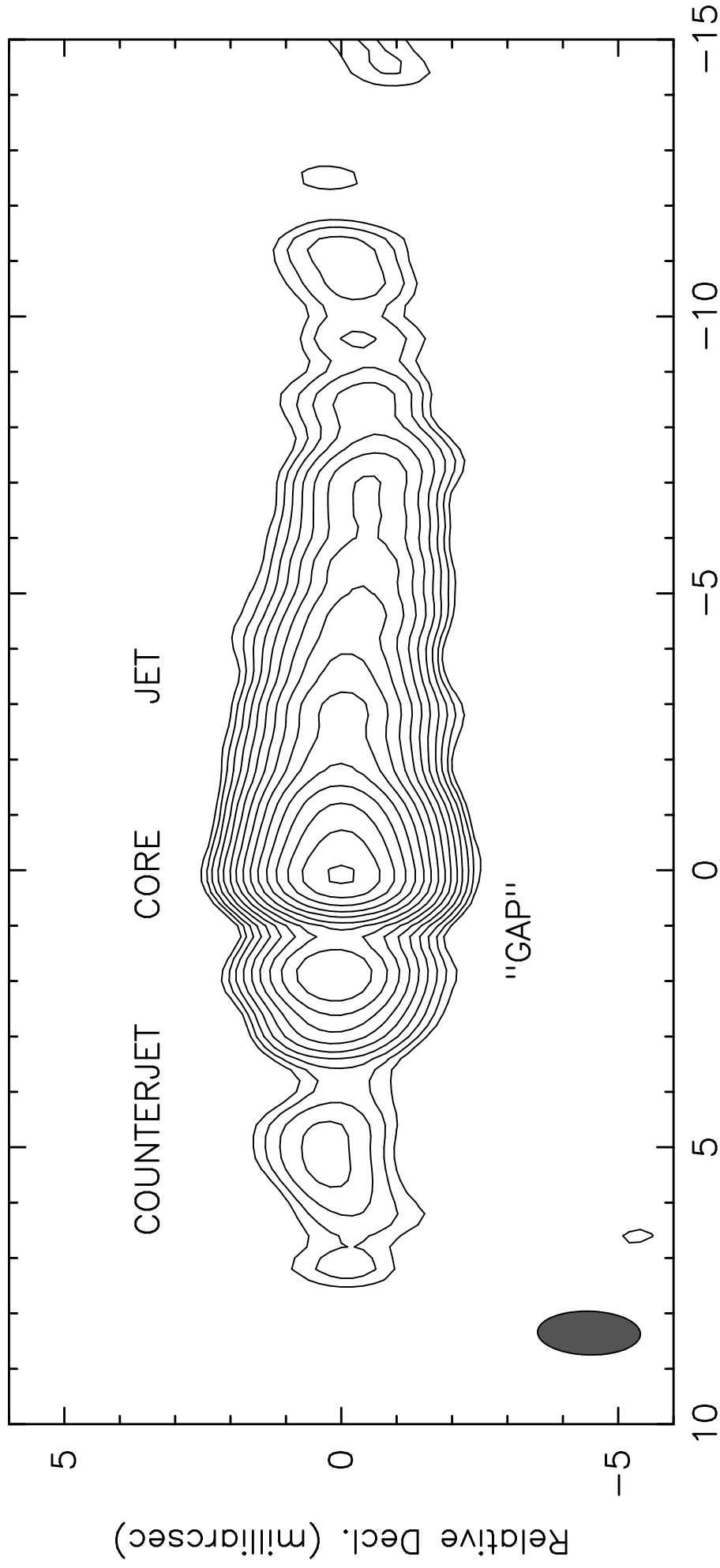
Our observations at 1.6 and 4.9 GHz appear to confirm the free-free absorption explanation for the sub-parsec radio morphology in NGC 4261. Measurements of the optical depth in the absorbed region and the distance between the absorption and the core as a function of frequency will allow the radial distribution of electron density in the inner parsec of the disk to be determined.

Acknowledgements. We gratefully acknowledge the VSOP Project, which is led by the Japanese Institute of Space and Astronautical Science in cooperation with many organizations and radio telescopes around the world. This research was carried out at the Jet Propulsion Laboratory, California Institute of Technology, under contract with the U.S. National Aeronautics and Space Administration.

References

Jones, D.L. & Wehrle, A.E. 1997, *ApJ*, **484**, 186

NGC 4261 8.387 GHz 01/04/95



Relative R.A. (milliarcsec)

